

Non-local-thermodynamical-equilibrium effects in the x-ray emission of radiatively heated materials of different atomic numbers

I. B. Földes,¹ K. Eidmann,² G. Veres,¹ J. S. Bakos,¹ and K. Witte²

¹*KFKI-Research Institute for Particle and Nuclear Physics, Association EURATOM, H-1525 Budapest, POB. 49, Hungary*

²*Max-Planck-Institut für Quantenoptik, D-85748 Garching, Germany*

(Received 22 December 2000; revised manuscript received 2 April 2001; published 26 June 2001)

X-ray self-emission of radiatively heated materials with different values of Z has been investigated. Thin foils were uniformly heated by a 120-eV *Hohlraum* radiation of 400-ps duration in order to study the self-emission of a homogeneous, optically thin material. The x-ray emission spectra were followed for more than 2 ns. The spectrally integrated emission shows not only a strong Z dependence, but different temporal behaviors for different values of Z . The lower is the value of Z of the x-ray heated matter, the longer is the duration of self-emission. Theoretical comparison with a hydrocode and FLY post-processing shows a non-local-thermal equilibrium behavior caused by direct photoionization due to the thermal pumping radiation, which has a higher brightness temperature than the matter temperature of the heated material.

DOI: 10.1103/PhysRevE.64.016410

PACS number(s): 52.25.Os, 52.38.Ph, 52.50.Jm, 42.55.Vc

I. INTRODUCTION

X-ray emission of radiatively heated matter is an issue of considerable importance especially for inertial confinement fusion (ICF). Homogeneous, thermal x-ray sources of several hundred eV in temperature [1] can be created in laser plasmas of high- Z materials by the effective conversion of high intensity laser radiation. *Hohlraum* targets allow us to generate intense, near Planckian radiation with brightness temperatures up to 300 eV [2]. Heating of matter by this radiation adds impact to ICF, where in the case of indirectly driven ICF [3] the conversion occurs inside a *Hohlraum* capsule made of high- Z (gold) material.

Another application is connected with the heating of thin foils for the purpose of opacity measurements. Thin foils are heated by thermal x rays so that fairly homogeneous temperature and density are generated, which provides a possibility to measure x-ray opacities [4,5].

Self-emission of x-ray heated matter is an important issue. In ICF the fusion capsule is heated by thermal x rays. While the use of high- Z material seems to be suitable for x-ray converters, the fusion capsule is best coated with a low- Z material that has low emission rates, and thus most of the energy is spent on the compression. Most recent works aimed at optimizing indirectly driven ICF by optimizing the conversion of laser radiation to x rays on the external wall of the cavity, and by improving the absorption of the fusion capsule by the choice of an optimized capsule ablator [6]. A possible source of the energy losses in the fusion capsule is reemission of the heating x rays [7,8]. Although capsules may reemit a considerable part ($\approx 50\%$) of the x-ray energy [7,9], most of the x rays are absorbed again and then reemitted on the cavity wall [10]. Therefore, its relative importance in a high- Q cavity is not very high. Indeed, most works on *Hohlraum* capsules simply neglect it [3,6], even if it is emphasized [6] that some percent of improvement in the total efficiency might be of considerable importance. Reemission of thick, low- Z foils was experimentally investigated in this context [9,11,12] and the results, especially as concerns the

albedo, were in fairly good agreement with the simulations, thus a scaling of the results up to fusion conditions became possible [9].

An important problem is however the deviation from the local thermal equilibrium (LTE). The shape of the experimentally measured spectra deviated from that of the simulations in some details. A small deviation between experiment and theory was found between the intensity ratio of H- and He-like C ions [9]. The relative weight of H-like lines found in the experiments is higher than expected from the simulations, which were carried out based on a LTE model. Note that the hydrocode [13] and the following post-processing use LTE opacities [9,14]. The deviation was therein attributed to non-LTE effects due to photoexcitation and photoionization. It was concluded [9] that deviations from LTE for the typical densities of $\rho = 0.1\text{-g/cm}^3$ (where most of the emission was emitted in the experiments) photoionization may increase the hydrogenlike level population with a factor of 10%, whereas the heliumlike level populations will decrease.

Non-LTE effects are also important in opacity studies carried out with thin foils, in which case only absorption is investigated. The simultaneous investigation of emission is a supplementary diagnostics which also gives information about the state of the foil, i.e., about deviations from LTE, by checking that to what degree absorption and emission fulfill Kirchhoff's law.

The aim of the present work is to study the emission of radiatively heated matter under conditions when non-LTE effects are present. Deviations from LTE are expected when the density of the heated material becomes small, while its temperature is sufficiently high. The interaction with a Planckian radiation field can bring the sample into the LTE state, but only if the interaction takes place for a sufficiently long time [1,15]. In this case collisions will no longer be dominant, as compared with photoionization and photoexcitation. This was kept in mind when thin foils were chosen with heated densities about two orders of magnitude lower than that mentioned above. It can be mentioned that most of previous works [16] on photoionization and photopumping

aimed to study line coincidences for x-ray laser pumping. In the present work the photoionization effect caused by a nearly Planckian radiation is studied. A concerning problem can also be addressed, i.e., whether a thermal x-ray source can be used for pumping x-ray lasers, although it might be less efficient [17].

In previous experiments [11,12,9] thick samples were heated by x rays from one side, and their emission was investigated from the same side but in the opposite direction along the normal of the heated foil. The observed spectra in this case was a result of emission from an inhomogeneous density and temperature distribution. Therefore, the spectra were modeled by solving the radiation transport equation after the density and temperature distributions were calculated by a hydrocode. Although heating by x rays gives a rather smooth density distribution and most of the emission occurs at a given density and temperature, the investigation of x-ray emission from a uniform layer is easier to understand. Another problem is that in the case of planar geometry [11] the source radiation is not quite Planckian, whereas in the case of *Hohlraum* geometry [12,9] one has only a limited temporal window for the observation because of the closure of the diagnostic hole and of cavity filling with gold plasma.

In order to carry out experiments with clean conditions we used in the present work a special type of *Hohlraum* capsule [18,19] which was well characterized in shock-wave experiments. The thickness of the emitter sample is chosen so that it is practically uniformly heated. The emitted radiation is observed parallel to the foil, i.e., altogether the emission of a uniformly heated layer with a considerable optical depth is investigated. In this geometry plasma filling of the cavity is not an important issue: no gold plasma will come into the line of the observation. Therefore, emission of the radiatively heated matter can be observed over a long duration, and consequently the temporal dependence of its emission can be well studied.

The appropriate thickness of the material was chosen after numerical simulations. The target foil must be heated uniformly early, at the beginning of the heating x-ray pulse. In order to investigate self-emission of materials with different values of Z , the thickness of the foils were chosen to be of equal areal mass density for different materials, thus providing similar conditions for the different materials. The thickness of the samples was chosen so that the characteristic density of the material was as low as 10^{-3} g/cm³ during most part of the emission. Experiments were carried out for the lowest Z material, carbon, with different initial thicknesses.

In Sec. II we describe the experimental setup and the shape of the targets and the emitter foils. Results of the temporally and spectrally resolved emission spectra are analyzed in Sec. III. In Sec. IV the experimental data are compared with the MULTI hydrocode and the FLY post-processor.

II. EXPERIMENTAL SETUP

The experiments were carried out with the third harmonics of the ASTERIX IV iodine laser (a 200-J, 400-ps light pulse of $0.44\text{-}\mu\text{m}$ wavelength). The laser beam was focused

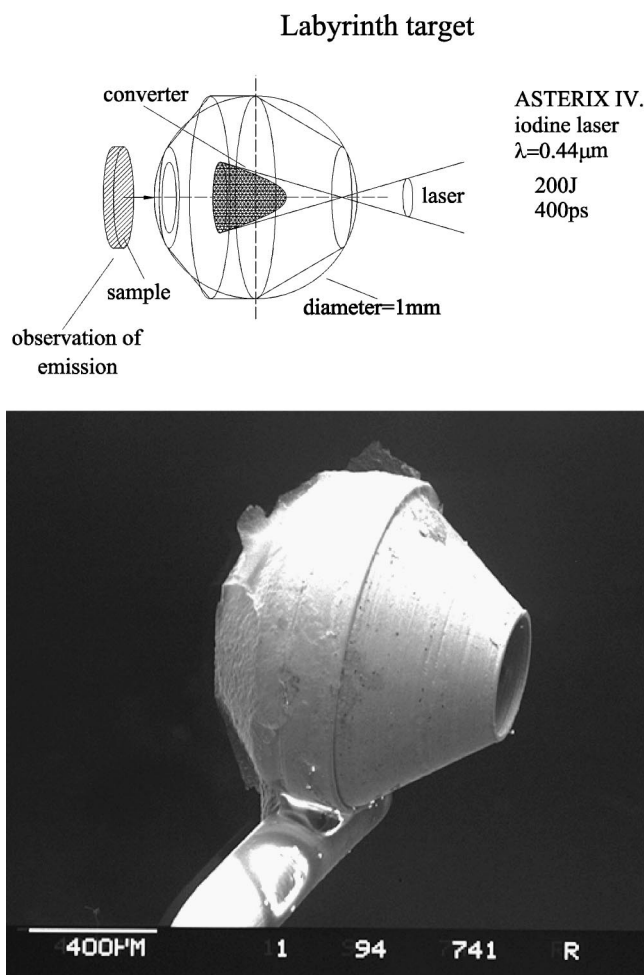


FIG. 1. Target-arrangement for the experiment (top) and a photograph of the target (bottom).

onto the target by an $f/2$ lens. The experimental arrangement is drawn in Fig. 1, and a photo of the target is also shown there.

The *Hohlraum* capsule used was a so called labyrinth type [18,20], where the primary laser pulse falls on a converter cone and does not directly strike the inner wall of the target. This results in a very homogeneous x-ray field, but with the drawback that this target is sensitive to the correct alignment. Poor alignment may cause the primary laser pulse to fall directly onto the emitter foil, which was fixed onto a diagnostic hole of $400\text{-}\mu\text{m}$ diameter on the rear side of the target. In the case of correct alignment, however, the shock-wave experiments [18,20] showed that a very homogeneous shock breakout occurs simultaneously in the whole area of the diagnostic hole, thus confirming the uniform heating at the whole plane of the target foil. The velocity of the shock-wave was directly measured to be 2.2×10^6 cm/s in Al [20], from which the temperature of the heating x rays can be easily determined to be 120 eV according to a simple scaling law [9]. It should be noted that shock-wave experiments are broadly used for temperature measurements in *Hohlraum* targets [2], and the temperatures derived with this method is in good agreement with the one obtainable from spectroscopy [9].

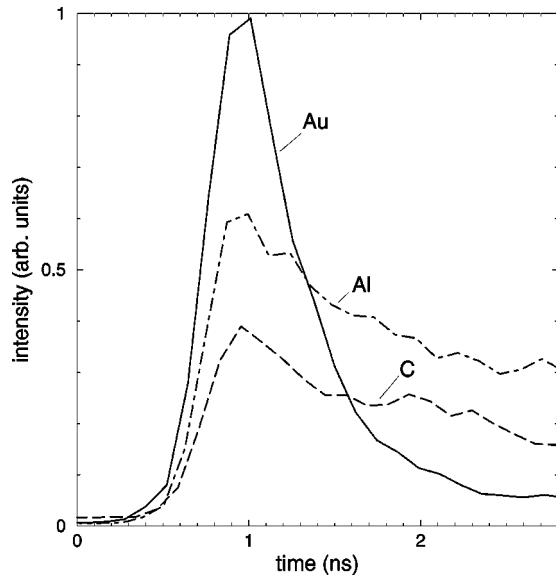


FIG. 3. The time dependence of x-ray emission from Au, Al, and C in a spectral range of 2–6 nm.

the weakness of the signal in this case, and probably not by the emission of, e.g., gold, because the emission is mostly featured by the strong Ly- α line until the late stage of emission, even at 2 ns after the time of maximal emission. At shorter wavelengths we can see the Ly- β ($1s-3p$) line and a recombination continuum. Carbon spectra will be discussed in more detail in subsequent sections.

An interesting finding of our observations is the time dependence of the emission of different materials. The time dependence of the emission of Au, Al, and C is shown in Fig. 3 after spectral integration in the 2–6-nm range. The emission of Au has a strong maximum, and then it decreases rapidly. Its duration is comparable to the laser pulse duration. However, the time dependence of Al has a slower decay in the emission, i.e., the emission is still approximately about 50% of the maximum value at 2 ns after the time of maximal emission. This slow decay is even more pronounced for the lowest Z material, carbon. It can be mentioned that the decay of Ag and Ti is somewhat slower than that of Au, but not as slow as for Al and for C.

Figure 4 shows the Z dependence of the total spectrally integrated radiation. The emission of Au was taken to be unity, i.e., the emission relative to gold is given here. The time integration was carried out until 1.0 ns after the peak of Au emission (the jitter was less than 100 ps). The relative strong total emission of carbon is caused by its slow decay; its emission increases from 30% of Au emission until 0.5 ns after the time of maximal emission to 45% until 1 ns (as seen in Fig. 4), and to 65% until 1.5 ns. That this long-lasting emission originates from carbon is confirmed by that in the observed spectra the most characteristic feature was always the Ly- α radiation.

A similar increase of the emission with Z was observed previously by Nishimura *et al.* [11] for elements of higher Z . Those experiments were carried out with emitters of larger density, aiming for conditions relevant for ICF.

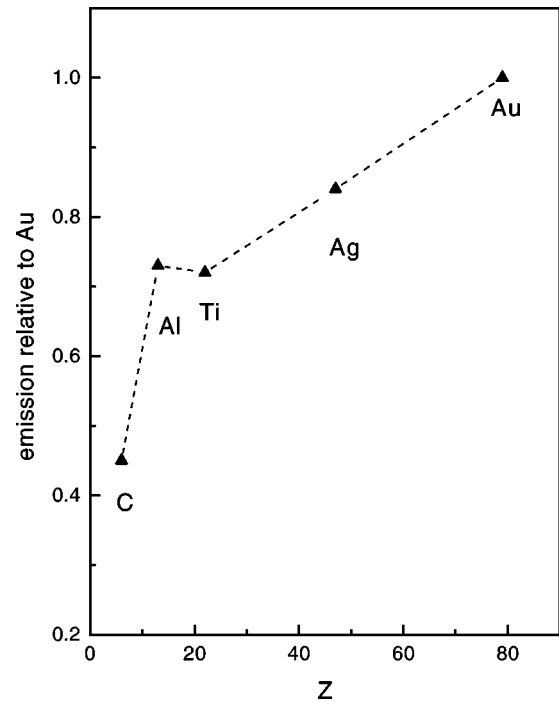


FIG. 4. Temporally integrated emission of different materials as compared to gold. The time integral was carried out until 1 ns after the peak of maximal emission in an integrated spectral range of 2–6 nm.

IV. DISCUSSION

Numerical simulations were carried out by using the MULTI hydrocode [13]. MULTI is a one-dimensional code, which describes the radiation transport by a multigroup diffusion approximation. Radiative opacities for the simulations were served by the SNOP code [23]. The calculations were carried out with a squared sinusoidal Planckian pumping x-ray pulse [$\propto \sin^2(\pi t/2\tau)$] of 500-ps full width at half maximum (FWHM) duration. As we consider the heating of a certain surface element of the Hohlraum target it must be kept in mind that it is heated by the radiation of the other surface elements, which might have different temperatures because the target optimization aims to keep constant just the temperature of the part to be investigated. Therefore, the heating radiation is averaged over the whole surface visible to the sample. If the internal surface of the Hohlraum target is uniformly heated and there is no direct laser spot, it is possible to measure directly the x-ray source flux and the corresponding temperature at any (Au) wall elements [24]. In the case of the present labyrinth target, the sample does not “see” direct laser spots; the surface elements visible to the sample are not necessarily of the same temperature, and their distance from the sample can also differ. It is just the sample that has a uniform temperature. Even in this case and similar cases, we can well rely on the simulations which derive the time-dependent heating pulse from the agreement between the time dependence of the gold sample spectra for various pumping sources [24]. As discussed previously in detail [9,12,14] when comparing simulations with experimental data obtained with the GEKKO XII and Asterix lasers, the

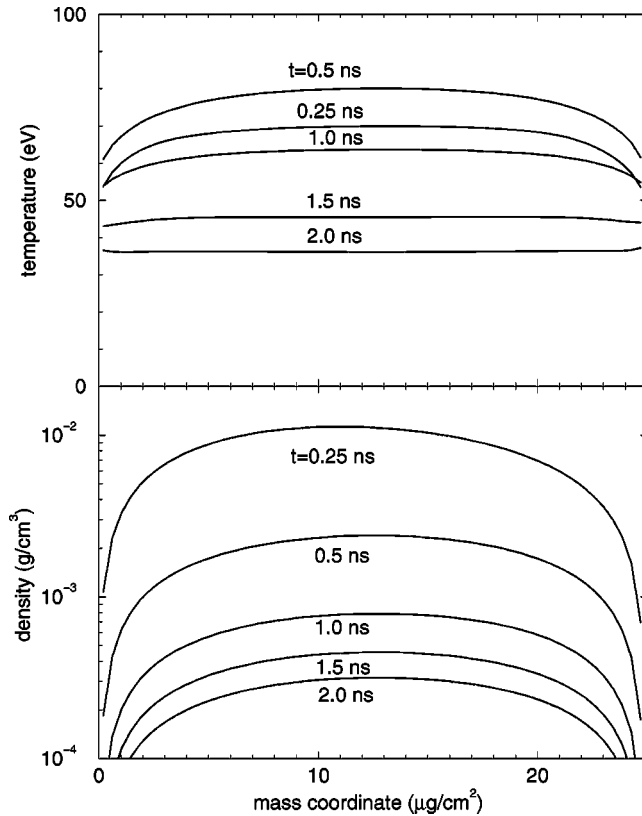


FIG. 5. Time evolution of temperature and density distribution of a $25\text{-}\mu\text{g}/\text{cm}^2$ carbon foil as calculated by the MULTI hydrodynamic code. The foil is irradiated from the left hand side by isotropic Planckian x rays at a temperature of 120 eV and a FWHM of 0.5 ns; $t=0$ ns corresponds to the peak of the heating pulse.

x-ray pulse may have asymmetry, and its total duration may be somewhat ($\approx 20\%$) longer than the laser pulse itself. A recent paper [25] dealt with the pulse shape in detail, and claimed a pulse duration for the asymmetric x-ray pulse that is twice as long as the laser pulse. The experimentally obtained gold emission in our case was fairly symmetric; therefore we remained at a symmetric pumping pulse throughout this work.

Figure 5 shows the temperature and density distributions for a $25\text{-}\mu\text{g}/\text{cm}^2$ carbon foil at different time steps as given by MULTI. We can see that soon after switching on the heating pulse, i.e., well before its peak, both distributions begin to become uniform, with the temperature increasing until the maximum of the heating pulse. The results of simulations with different target thicknesses show that the layer heated by the 120-eV thermal x-ray pulse becomes uniformly heated within the first 250 ps, i.e., during the rising of the heating pulse, if the thickness is kept below a $80\text{-}\mu\text{g}/\text{cm}^2$ thickness. They also show that the size ($\approx 80\%$ of the total material) of the expanding foil remains below $200\ \mu\text{m}$ in the first nanosecond and below $400\ \mu\text{m}$ in the second nanosecond. This means that in our perpendicular observation direction the emitter remains nearly one dimensional, and the small source size provides a fairly good resolution.

We can see that the temperature increases within a quarter ns up to nearly 70 eV, with a density less than $10^{-2}\ \text{g}/\text{cm}^3$.

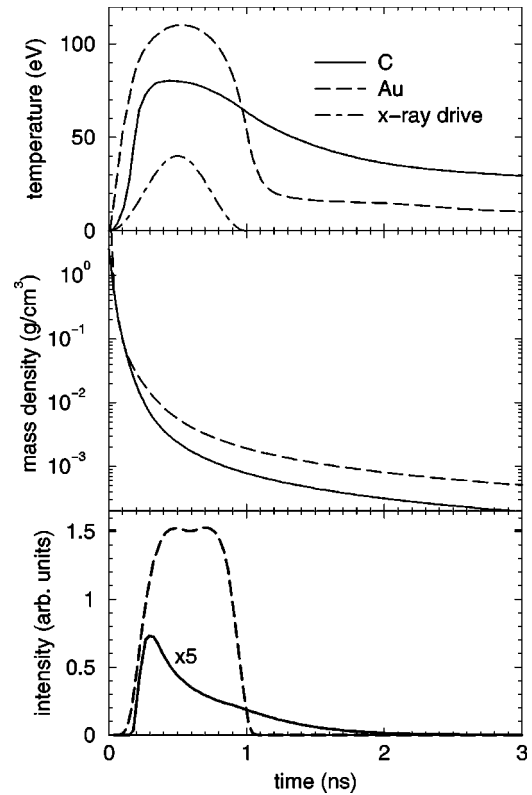


FIG. 6. Time evolution of the averaged electron temperature, density, and emitted intensity for a $25\text{-}\mu\text{g}/\text{cm}^2$ -thick C layer, and for $15\text{-}\mu\text{g}/\text{cm}^2$ Au on a $9\text{-}\mu\text{g}/\text{cm}^2$ C layer heated by 120-eV thermal x rays calculated by MULTI. The dash-dotted line illustrates the shape of the heating x-ray pulse.

The maximum temperature remains lower than 80 eV because, with increasing temperature, the foil becomes more and more transparent to the heating x rays. The density of the heated matter drops down to $10^{-3}\ \text{g}/\text{cm}^3$ by the peak of the heating pulse.

As a consequence of the uniformity it is reasonable to treat the foil as a material with a single (averaged) value of density and temperature. The hydrodynamical behavior was similar for the different materials, as e.g., even Au becomes uniform soon as the heating pulse rises. The time evolutions of the averaged electron temperature and density for gold and carbon are compared in Fig. 6. Evidently, the matter temperature for both Au and C remains below the brightness temperature of the heating radiation. Heating increases the temperature of the foil, which tends to reach thermal equilibrium at a material temperature equal to the brightness temperature of the radiation during a long enough time. In the present case the optical thickness of the material is low and the heating is not effective enough; thus the temperature of the foil will not reach the brightness temperature of the heating radiation during the time of heating. Au has a higher value as Z , and consequently a higher opacity; that is why higher matter temperature is obtained for Au than for C. It can be clearly seen that a high- Z material (gold) cools down faster which is attributed to the stronger radiation cooling in high- Z matter. The emission of Au, as calculated by SNOP [23] shows a pulse duration roughly equal to the heating

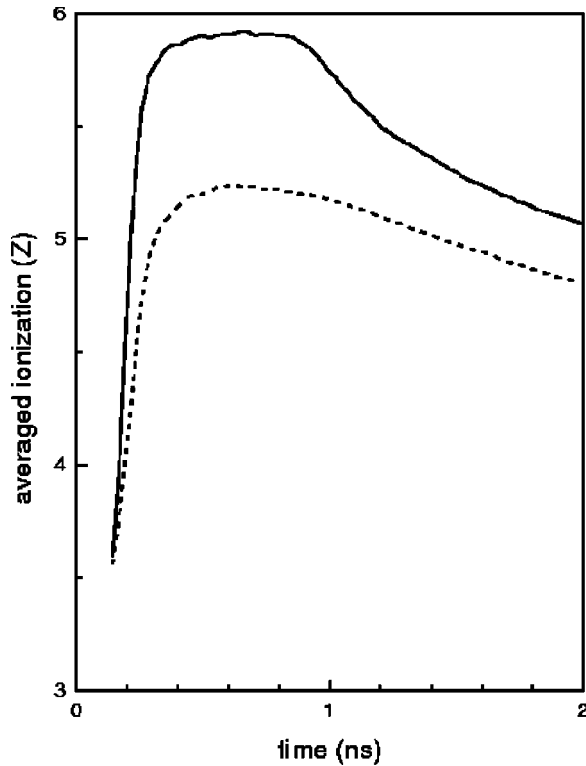


FIG. 7. Averaged ionization of $25\text{-}\mu\text{g}/\text{cm}^2$ -thick carbon. MULTI simulations with a $120\text{-eV}\sin^2$ heating pulse, post-processed by FLY. The models of FLY were the time-dependent model with radiation pumping taken into account (solid line), and with direct radiation pumping neglected (dashed line).

pulse, in agreement with the experiments. Carbon emission, however, decreases significantly more quickly than observed in the experiments, and its maximum (note that in order to show it in more detail it was multiplied by a factor of 5 in Fig. 6) is also significantly lower than the one observed. Consequently the time integrated emission was calculated to be only about 10% of that of Au, in contrast to the observed high value of Fig. 4.

Therefore, it seems necessary to carry out calculations with a non-LTE model. In order to study non-LTE effects caused by the low density of the matter and by the external radiation source, the FLY code [26] was used for post-processing the hydrodynamic data given by MULTI. The FLY code [26] can be used to analyze non-LTE effects. It solves the time-dependent rate equations for elements of Z being between 2 and 26 in order to determine the populations of the different excitation and ionization states. An external radiation source can also be included.

The averaged ionization Z of the $25\text{-}\mu\text{g}/\text{cm}^2$ carbon layer is illustrated in Fig. 7, as given by FLY, comparing the results of the time-dependent rate equations with and without the heating radiation taken into account. It is evident that the ionization rate of carbon is strongly underestimated if the thermal heating radiation of the material is neglected. It is just direct photoionization and photoexcitation which result in a higher Z . The direct interaction with the heating radiation heats up the matter until it approaches thermal equilibrium. Note that our approach is only an approximation in

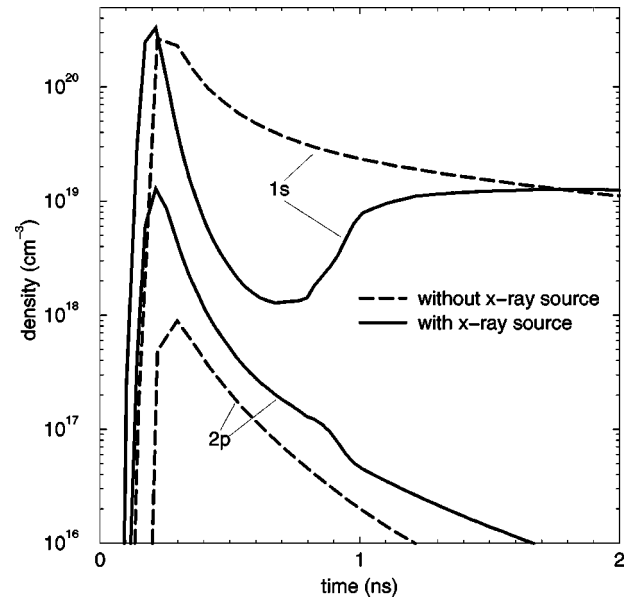


FIG. 8. Calculated populations of the $1s$ and $2p$ levels of C^{5+} for a $25\text{-}\mu\text{g}/\text{cm}^2$ -thick carbon foil with (solid line) and without radiation pumping taking into account (dashed line).

order to illustrate these effects, because the hydrocode itself uses the LTE approximation. The effect of radiation is even stronger on the level populations, as illustrated in Fig. 8, where the populations of the $n=2$ and 1 levels are shown with and without heating radiation. The effect of radiation is that the population of the $n=2$ level increases by approximately an order of magnitude, whereas that of the $n=1$ level is depleted. The effect of photoionization is that part of the C^{5+} ions will be fully ionized, reducing the total number of line-radiating ions. However, this effect is smaller than the increase of the $n=2$ level population increase; therefore, strong emission is expected to be caused by radiation pumping.

Figure 9 illustrates the carbon spectra as calculated by FLY with and without radiation pumping taken into account at the time of maximum emission. Its main effect—as expected—is an increase of the emission. As to the spectral structure of emission, we must note here that line radiation only from the Ly- α and Ly- β lines can be distinguished; the Ly- γ line already merges into the continuum, in good agreement with the experiments. The strong Ly- α radiation can be attributed to the process of direct photoionization and photoexcitation. At these low densities the effect of collisions will be reduced, and direct interaction with the external thermal radiation field must be taken into account.

The temporal behavior of carbon emission is illustrated in detail in Fig. 10, where a spectral integration is carried out from 200- to 600-eV photon energies both for the experimental and theoretical data calculated by the FLY postprocessor. We can see that the rise of the pulse and its shape around the maximal emission are well reproduced by the calculations (better than that with the LTE model in Fig. 6). However, there is a considerable deviation between the calculations and the observations at the decay of the pulse, where the calculations suggest a faster decay than the observed

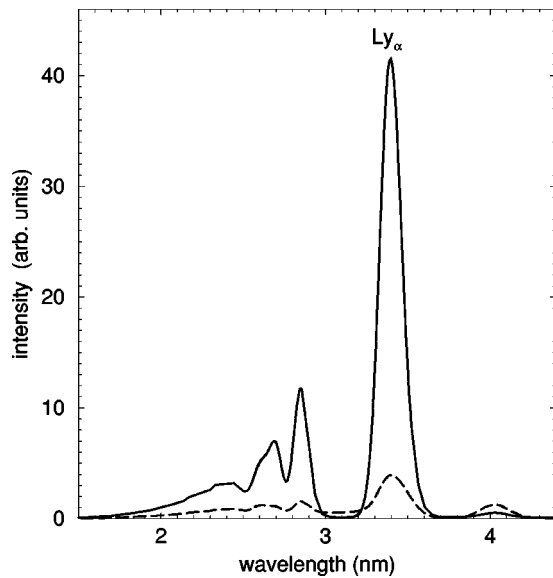


FIG. 9. Calculated carbon spectrum with (solid line) and without direct radiation pumping taken into account (dashed line).

slow decay of x-ray emission. This disagreement cannot be explained even if changing the atomic model in FLY. It seems as if the source radiation in the Hohlraum target had a longer duration than the 500 ps used throughout the calculation. However, a longer pulse duration contradicts the observed shorter decay of gold emission. Thus, although the simulations (Fig. 6) agree with the emission time of carbon being longer than that of gold, they do not reproduce the observed slow decay of carbon emission in detail.

The results for Al foil proved to be a good example to illustrate radiative pumping effects, which can be done by comparing the obtained spectroscopical results with FLY calculations of the averaged ionization Z . Figure 11 compares the calculations with and without radiation pumping taken into account. If we neglect direct radiation in the time-

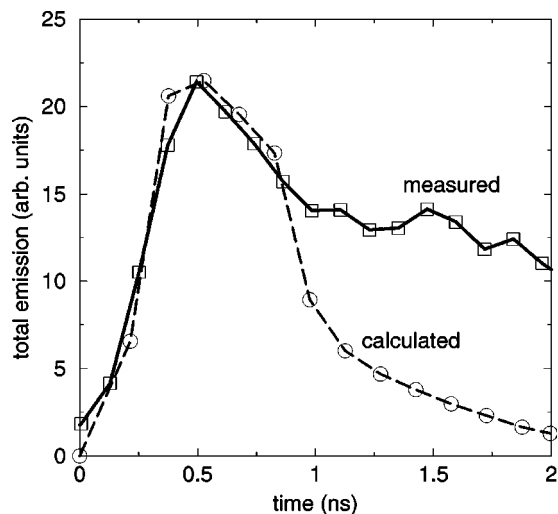


FIG. 10. Time dependence of the emission of a $25\text{-}\mu\text{g}/\text{cm}^2$ -thick carbon after spectral integration from 200 to 600 eV as given by experiment (solid line, squares) and theory (dashed line, circles).

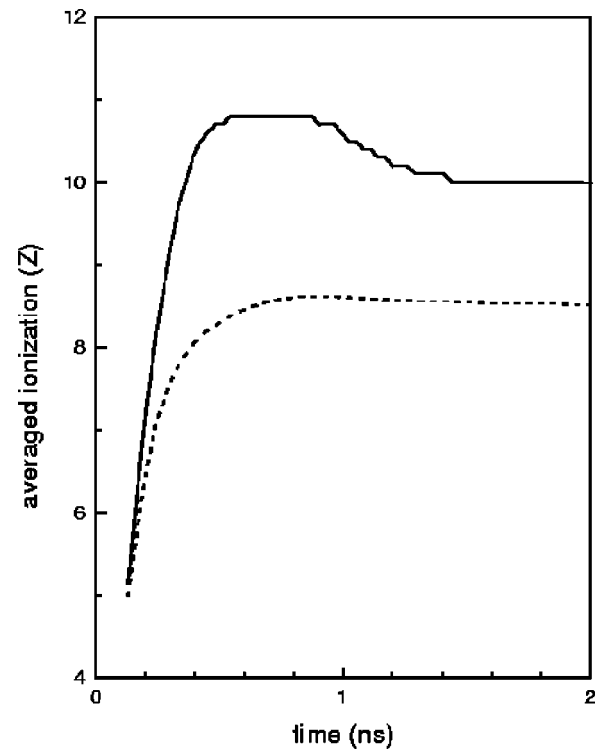


FIG. 11. Averaged ionization of Al on C. MULTI simulations with a 120-eV sinusoidal heating pulse, post-processed by FLY. The models of FLY were the time-dependent model with radiation pumping taken into account (solid line), and with direct radiation pumping neglected (dashed line).

dependent FLY calculations, the calculated Z value is as low as 8 all the time, significantly lower than expected from the observed spectra, where dominating radiation from Al^{9+} and Al^{10+} ions were observed. The long-lasting high ionization state is in agreement with the experiments, which showed that strong lines of Al^{10+} are present until at least 0.5 ps after the peak of emission, whereas Al^{9+} lines remain strong until more than 1 ns after the time of the peak emission. Thus we can see that the observed spectra, which is dominated until this late time by Al^{9+} and Al^{10+} , can only be explained by the effect of direct photoionization taken into account.

One of the driving ideas for the present investigation was the eventual use of thermal radiation for x-ray laser pumping. It is well known that photoionization may lead to a depletion of the ground state and to a photoionization laser [27]. Its possibilities for a carbon Ly- α laser was discussed for the case of monochromatic pumping by Goodwin and Fill [17], where it was mentioned that monochromatic pumping is more efficient than thermal pumping. However, if one has an intense Planckian pumping source with a spectral maximum near the ionization potential of C^{5+} , as is the case with 100–120-eV radiation, the expectations can be similar because the shape of the Planckian spectrum drops rather fast for lower photon energies, i.e., most of it can well be used for pumping. Thus the photoionization probability of the $n=2$ levels by this radiation is significantly lower than that of the $n=1$ levels according to Kramers' law [28]. Our calculations with the FLY code show—in agreement with the pre-

vious detailed work [17]—that in order to obtain inversion, the material temperature must be kept as low as 10 eV before “switching on” the pump radiation. Also, the required intensity is significantly higher (10^{15} W/cm²) than the intensity corresponding to the 120-eV brightness temperature. Therefore, the realization of this laser scheme with a Planckian pumping does not seem probable in the next future.

V. CONCLUSION

Experiments were carried out to study the self-emission of radiatively heated thin foils. It was found—according to expectations—that materials of higher values of Z emit more strongly than low- Z materials. Low- Z materials however emit for a longer time; therefore, the difference between time-integrated emission decreases with time. The experimental results were compared with MULTI simulations both with SNOP and FLY post-processing. The observed emission of the low- Z materials was stronger and of longer duration than given by the calculations. The reason for this deviation could not well be explained.

The experiments were carried out on low-density foils in order to study the radiative pumping. The density was so low that it became transparent for the heating radiation, i.e., it became optically thin. Consequently the temperature remained significantly lower than that of the temperature of the heating radiation; therefore no equilibrium with the heating

radiation could be established. The observed high ionization state of carbon and aluminum can be attributed to non-LTE effects when it is heated by a Planckian radiation with a brightness temperature significantly exceeding the material temperature of the heated optically thin foil. Probably direct photoionization and photoexcitation causes a higher ionization of the low- Z matter. Thus even if the material is heated by thermal radiation, it might be in a non-LTE state if there is not enough time for the material to reach the brightness temperature of the heating radiation. It is also concluded that for the photoionization laser [27] on the carbon Ly- α line a monochromatic pumping source [17] is still preferred.

The thin carbon foil was nearly fully ionized by the high-temperature radiation; therefore the non-LTE effects were difficult to be observed. The photopumping effect were therefore stronger in the case of Al. The observed long-lasting high ionization state observed in aluminum draws attention to the importance of photoionization and photoexcitation.

ACKNOWLEDGMENTS

This work was supported by the PECO project of the European Community (Grant No. ERD-CIPD CT94-0083) and the Hungarian OTKA Foundation (Grant Nos. T07254 and T023526).

-
- [1] R. Pakula and R. Sigel, *Phys. Fluids* **28**, 232 (1985); **29**, 1340 (1986).
- [2] R.L. Kauffman, L.J. Suter, C.D. Darrow, J.D. Kilkenny, H.N. Kornblum, D.S. Montgomery, D.W. Phillion, M.D. Rosen, A.R. Theissen, R.J. Wallace, and F. Ze, *Phys. Rev. Lett.* **73**, 2320 (1994).
- [3] J. Lindl, *Phys. Plasmas* **2**, 3933 (1995).
- [4] P.T. Springer, D.J. Fields, B.G. Wilson, J.K. Nash, W.H. Goldstein, C.A. Iglesias, F.J. Rogers, J.K. Swenson, M.H. Chen, A. Bar-Shalom, and R.E. Stewart, *Phys. Rev. Lett.* **69**, 3735 (1992).
- [5] G. Winhart, K. Eidmann, C.A. Iglesias, A. Bar-Shalom, E. Minguez, A. Rickert, and S.J. Rose, *J. Quant. Spectrosc. Radiat. Transf.* **54**, 437 (1995).
- [6] L. Suter, J. Rothenberg, D. Munro, B. Van Wontherghem, and S. Haan, *Phys. Plasmas* **7**, 2092 (2000).
- [7] M. Murakami and J. Meyer-ter-Vehn, *Nucl. Fusion* **31**, 1315 (1991).
- [8] M. Basko, *Phys. Plasmas* **3**, 4148 (1996).
- [9] K. Eidmann, I.B. Földes, Th. Löwer, J. Massen, R. Sigel, G.D. Tsakiris, S. Witkowski, H. Nishimura, Y. Kato, T. Endo, H. Shiraga, M. Takagi, and S. Nakai, *Phys. Rev. E* **52**, 6703 (1995).
- [10] R. Pakula and R. Sigel, *Z. Naturforsch. Teil A* **41**, 463 (1986).
- [11] H. Nishimura, H. Shiraga, H. Takabe, Y. Kato, S. Miyamoto, M. Takagi, T. Norimatsu, T. Yamanaka, T. Jitsuno, M. Nakatsuka, S. Nakai, T. Endo, M. Murakami, T. Kanabe, and C. Yamanaka, in *Proceeding of the 14th International Conference on Plasma Physics and Controlled Nuclear Fusion Research, Würzburg, Germany, 1992* (IAEA, Vienna, 1993), Vol. 3, pp. 97–103.
- [12] I.B. Földes, K. Eidmann, Th. Löwer, J. Massen, R. Sigel, G.D. Tsakiris, S. Witkowski, H. Nishimura, T. Endo, H. Shiraga, M. Takagi, Y. Kato, and S. Nakai, *Phys. Rev. E* **50**, R690 (1994).
- [13] R. Ramis, R.F. Schmalz, and J. Meyer-ter-Vehn, *Comput. Phys. Commun.* **49**, 475 (1988).
- [14] I.B. Földes and K. Eidmann, *Laser Part. Beams* **14**, 487 (1996).
- [15] P.T. Springer, K.L. Wong, C.A. Iglesias, M.J. Hammer, J.L. Porter, A. Toor, W.H. Goldstein, B.G. Wilson, F.J. Rogers, C. Deeney, D.S. Dearborn, C. Bruns, J. Emig, and R.E. Stewart, *J. Quant. Spectrosc. Radiat. Transf.* **58**, 927 (1997).
- [16] C.A. Back, C. Chenais-Popovics, and R.W. Lee, *Phys. Rev. A* **44**, 6730 (1991).
- [17] D.G. Goodwin and E.E. Fill, *J. Appl. Phys.* **64**, 1005 (1989).
- [18] Th. Löwer *et al.*, in *Proceeding of the 16th International Conference of Plasma Physics and Controlled Nuclear Fusion Research, Montreal, 1996* (IAEA, Vienna, 1997), p. 107.
- [19] Th. Löwer, V.N. Kondrashov, M. Basko, A. Kendl, J. Meyer-ter-Vehn, R. Sigel, and A. Ng, *Phys. Rev. Lett.* **80**, 4000 (1998).
- [20] M. Basko, Th. Löwer, V.N. Kondrashov, A. Kendl, R. Sigel, and J. Meyer-ter-Vehn, *Phys. Rev. E* **56**, 1019 (1997).
- [21] B.L. Henke, P. Lee, T.J. Tanaka, R.L. Shimabukuro, and B.K. Fujikawa, *At. Data Nucl. Data Tables* **27**, 1 (1982).
- [22] P. Celliers and K. Eidmann, *Phys. Rev. A* **41**, 3270 (1990).

- [23] K. Eidmann, *Laser Part. Beams* **12**, 223 (1994).
- [24] H. Nishimura, Y. Kato, H. Takabe, T. Endo, K. Kondo, H. Shiraga, S. Sakabe, T. Jitsuno, M. Takagi, C. Yamanaka, S. Nakai, R. Sigel, G.D. Tsakiris, J. Massen, M. Murakami, F. Lavarenne, R. Fedosejevs, J. Meyer-ter-Vehn, K. Eidmann, and S. Witkowski, *Phys. Rev. A* **44**, 8323 (1991).
- [25] W. Pei, T. Chang, G. Wang, X. Zhang, C. Sui, and J. Zhang, *Phys. Plasmas* **6**, 3337 (1999).
- [26] R.W. Lee, *J. Quant. Spectrosc. Radiat. Transf.* **40**, 561 (1988).
- [27] M.A. Duguay and P.M. Rentzepis, *Appl. Phys. Lett.* **10**, 350 (1967).
- [28] Ya.B. Zel'dovich and Yu.P. Raizer, *Physics of Shock Waves and High-Temperature Hydrodynamic Phenomena* (Academic Press, New York, 1966).